Technical Memo

ECMWF
European Centre for Medium-Range Weather Forecasts

895

Calculating the Cosine of the Solar Zenith Angle for Thermal Comfort Indices

C Brimicombe, T Quintino, S Smart, C Di Napoli ,

R Hogan, H L Cloke and F Pappenberger

April 2022

Series: ECMWF Technical Memoranda

A full list of ECMWF Publications can be found on our web site under:

http://www.ecmwf.int/publications/

Contact: library@ecmwf.int

European Centre for Medium Range Weather Forecasts
Shinfield Park, Reading, Berkshire RG2 9AX, England

Abstract:

The cosine of the solar zenith angle (cossza) is a key component in Mean Radiant Temperature (MRT). Mean Radiant Temperature is used in the calculation of the Universal Thermal Climate Index (UTCI) and can be used in the calculation of Globe Temperature a component of the Wet Bulb Globe Temperature (WBGT), both of which are important thermal comfort and heat stress indices. It has previously been demonstrated that in numerical weather prediction services cossza should be integrated over a time step for the most accurate results. Here, we present the comparison of the operational cossza being used to create ERA5-HEAT, an instantaneous approach and a Gauss-Legendre Integration cossza. We further calculate MRT and UTCI for the ERA5-HEAT method and the methodology in the *thermofeel* library and see discrepancies in the approaches of on average -1.5K for MRT and -0.42K for UTCI. We suggest that the methodology in the *thermofeel* library supersedes the operational c code and is published alongside the existing ERA5-HEAT dataset in addition to forecast data being published, for users to make their own comparisons and extend this data's usefulness. We also suggest that a sensitivity analysis of the UTCI is carried out to aid better understanding of this thermal comfort index.

Introduction

The cosine of the solar zenith angle (cossza) is the angle between the sun's rays and the vertical (Aktaş & Kirçiçek, 2021). It is a key component in the calculation of mean radiant temperature (MRT), (Di Napoli et al., 2020; Vanos et al., 2021) which is used to calculate other thermal and heat indexes such as the Universal Thermal Climate Index (UTCI) (Fiala et al., 2012; Di Napoli et al., 2021) and the Globe Temperature component of Wet Bulb Globe Temperature (WBGT) (De Dear, 1987; Guo et al., 2018). In addition, MRT has been shown to be a better predictor of mortality than air temperature (Ta) which is one of the main impacts of extreme heat (Thorsson et al., 2014).

Each heat index has its benefits and limitations for modelling human thermal comfort. It has been shown for operation forecasts (i.e ECMWF) the most accurate version of cossza is a numerical integration over a forecast time step (Hogan & Hirahara, 2016). Different approaches to provide a cossza over a time step can be employed. These include integration methods as well as a simpler instant cossza.

Here we provide an overview of the current operational method for using cossza. Cossza is part of the ERA5-HEAT dataset (Di Napoli et al., 2021). We further compare this to an instantaneous method and a Gauss-Legendre Quadrature approximation of an integral, available as part of the new python thermal comfort library *thermofeel (Brimicombe, et al.,*

2021, 2022). This allows us to make recommendations for both *thermofeel* (Brimicombe, et al., 2021, 2022) and ERA5-HEAT (Di Napoli et al., 2021).

Methods

To calculate the cossza there are a number of different approaches that can be taken because an instantaneous cossza (hereafter instant) is required for the exact recorded time of the observation. Whereas using numerical weather prediction services leads to the requirement to calculate the integrated average cossza over a time step period, to have an accurate cossza. As such *thermofeel* provides both an instant cossza and an integrated cossza.

Instant cossza

Instant cossza is the simplest approach to calculating a cossza, it is calculated using equation 1 and 2 (Hogan & Hirahara, 2015, 2016). It involves the solar declination angle which is the angle between the equator and the center of the earth the center of the sun. In addition, it involves the local solar time.

$$\mu_0 = \sin\delta \sin\phi + \cos\delta \cos\phi \cos h \quad [1]$$

δ is the solar declination angle and ϕ is latitude, h is the local hour angle.

$$h = T + \lambda + \pi \quad [2]$$

T is local solar time and λ is longitude.

Integrated cossza

Integrated cossza is the method currently used in operations at ECMWF to calculate the ERA5-HEAT dataset it can be summarized by equation 3 (Hogan & Hirahara, 2015, 2016). It also takes into account sunrise and sunset when the value of cossza reduces to zero.

$$\overline{\mu_{0m}} = \sin\delta \sin\phi + \frac{\cos\delta \cos\phi \,(\sin h_{max} - \sin h_{min})}{h_{max} - h_{min}} \quad [3]$$

δ is the solar declination angle and ϕ is latitude, h_{max} is the end time of a time step and h_{min} is the beginning time of the time step.

Gauss-Legendre Quadrature integrated cossza

An accurate way to reduce the cost to a computer, in terms of computational power and time taken of integrating a cossza is to use an approximate numerical integration method and apply it to an instant cossza. Empirical experiments were carried out to compare Gauss-Legendre Quadrature to a Simpsons integral rule and Gauss-Legendre Quadrature chosen because it incurs in less redundant calculations when called over multiple time steps, since it does not evaluate the function at the interval boundaries(Zienkiewicz et al., 2005; Babolian et al., 2005; Goldstein, 1965). The Gauss-Legendre Quadrature is outlined in equation 4 where f(x) is equation 1 and visually in figure 1. ξ is the i-th coordinate of interval boundaries at which the function for cossza instant is evaluated and ω is the i-th weight factor for the numerical integral corresponding to the i-th coordinate.

$$\int_{h_{min}}^{h_{max}} f(x)dx \approx \frac{h_{max} - h_{min}}{2} \sum_{i=1}^{n} \omega_i f\left(\frac{h_{max} - h_{min}}{2}\xi_i + \frac{h_{min} + h_{max}}{2}\right) \quad [4]$$

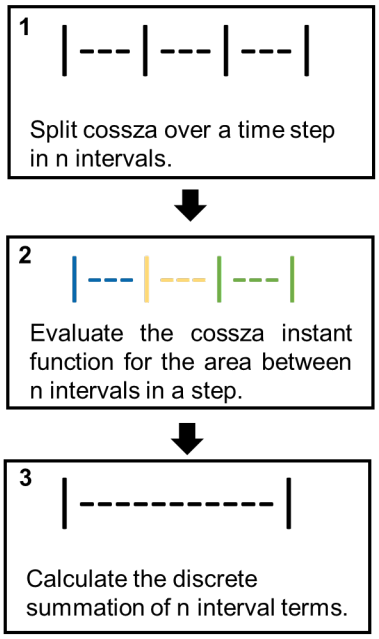

Figure 1: a schematic outlining the steps (1 to 3) taken to calculate a discrete summation integrated cossza using the instant cossza method (I.e., the distinct colours in step 2) in combination with the Gauss-Legendre quadrature approximation.

Mean Radiant Temperature

The mean radiant temperature can be defined as the incidence of radiation on a body. For a numerical weather prediction service, it requires 5 input radiations (surface-solar-radiation-downwards, surface net solar radiation, total sky direct solar radiation at surface, surface

thermal radiation downwards, surface net thermal radiation) in addition to the cosine of the solar zenith angle (cossza). The full methodology for mean radiant temperature is available in Di Napoli et al., 2020 and is summarized in table 1 and equations 5 and 6.

$$\mathrm{MRT}^{*} = \frac{1}{\sigma}\left\{ \mathrm{f_a}\, \mathrm{L}_{\mathrm{surf}}^{\mathrm{dn}} + \mathrm{f_a}\, \mathrm{L}_{\mathrm{surf}}^{\mathrm{up}} \left[\frac{\mathrm{a_{ir}}}{\varepsilon_{\mathrm{p}}} + \left(\mathrm{f_a}\, \mathrm{S}_{\mathrm{surf}}^{\mathrm{dn,diffuse}} + \mathrm{f_a}\, \mathrm{S}_{\mathrm{surf}}^{\mathrm{up}} + \mathrm{f_p}\, \mathrm{I}^{*} \right) \right] \right\}^{0.25} \quad [5]$$

$$\mathrm{f}_p = 0.308 \cos\left(\gamma \left(\frac{0.998 - \gamma^2}{50000} \right) \right) \quad [6]$$

Table 1: The radiation variables that are used in the calculation of the MRT in Equations 5 and 6. Table 1 from Di Napoli et al., 2020

Name	Symbol/Equation
Surface solar radiation downwards	S_{dnsurf}=$S_{dn,directsurf}$+$S_{dn,diffusesurf}$Ssurfdn=Ssurfdn,direct+Ssurfdn,diffuse
Surface net solar radiation	$S_{netsurf} = S_{dnsurf} - S_{upsurf}$Ssurfnet=Ssurfdn−Ssurfup
Direct solar radiation at the surface	$S_{dn,directsurf}$Ssurfdn,direct
Surface thermal radiation downwards	L_{dnsurf} Lsurfdn
Surface net thermal radiation	$L_{netsurf}$=L_{dnsurf}−L_{upsurf}

A key component of Mean radiant Temperature is known as Istar this is defined as "*radiation intensity of the Sun on a surface perpendicular to the incident radiation direction"* (Di Napoli et al, 2020) in the current operational code this is calculated using equation 7. Where Direct Solar Radiation (dsrp) is available I* is equal to this variable.

$$I* = fdir \,/\, cossza \ (where\ cossza > 0.01)$$

[7]

Universal Thermal Climate Index

The UTCI is a bio-thermal comfort index which makes use of the meteorological parameters of 2m temperature, water vapour pressure, 10m wind speed and mean radiant temperature and a body model it is estimated by a 6-order polynomial which is summarized by equations 9 and 10 (Bröde et al., 2012; Fiala et al., 2012; Di Napoli et al., 2021).

$$UTCI(Ta, Tr, Va, Pa) = Ta + Offset(Ta, Tr, Va, Pa)$$

[9]

Where Ta= air temperature, Tr= mean radiant temperature, Va= wind speed Pa= water vapour pressure

$$Pa = Ps \times \frac{\varphi}{100}$$

[10]

Where Ps = Saturation Vapour Pressure and φ= relative humidity percent.

Results

The implementation of the integrated cossza (figure 2a) visually is different from the other cossza methods implemented, being clipped at the top of the parabola for the 42nd time step after the initial date of 21 May 2021.The difference between the integrated cossza and the Gauss-Legendre cossza is at most ±0.1° (Figure 2d).The instant cossza has the largest area with complete darkness indicated by 0° values in (figure 2c). In addition, visually the instant cossza covers a slightly different area than the integrated approaches (figure 2c). This is because it is for the instant time at the 42nd time step whereas the integrations are the average of step 39th to 42nd. Further, both the integrated cossza (figure 2a) and the Gauss-Legendre cossza (figure 2b) have a small gradient than the instant cossza (figure 2c) which can be seen in the color gradient in figure 2. This allows for sunset and sunrise to be considered more accurately because there is a greater range in cossza values between maximum sun and darkness.

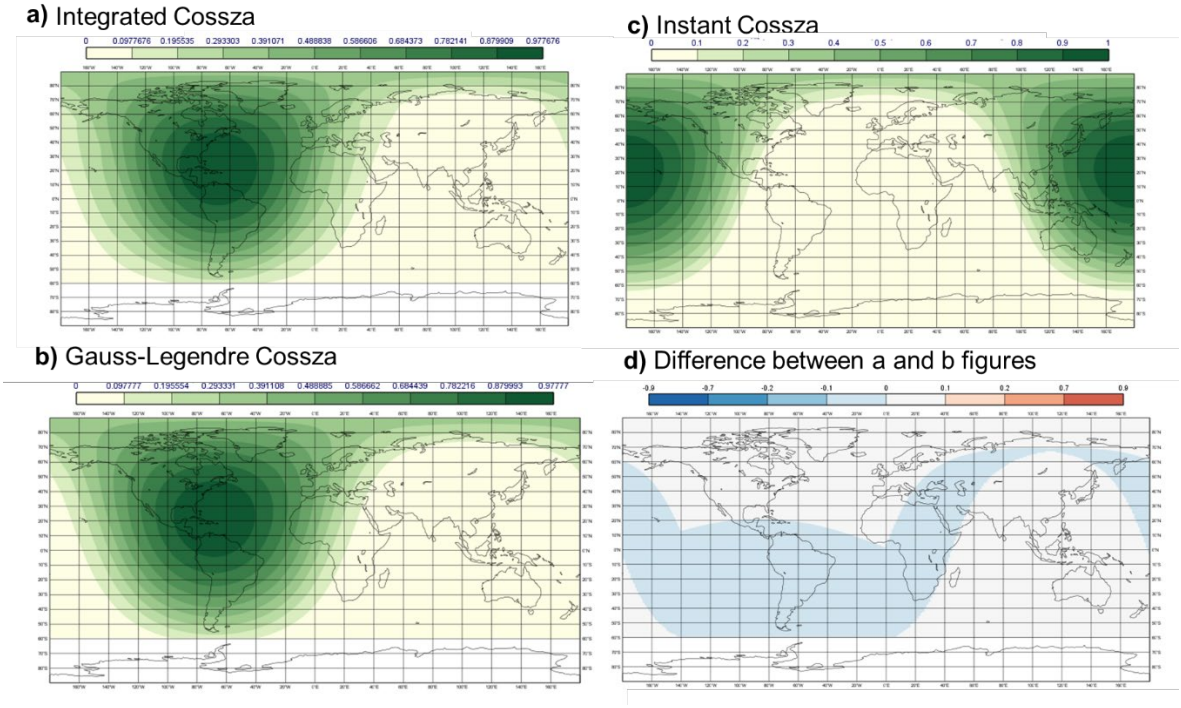

Figure 2: Showing the difference cossza approaches for 42hr lead time from 21 May on a 3 hour time step, a) the current operational (integrated) cossza for ERA5-HEAT calculated in the c coding language, b)an average of an gaussian integration of the instant cossza for a time step, c) an Instant cossza for a given hour and d) the difference between parts a and b of this figure.

The biggest difference is more than +10K between the operational MRT (figure 3a) and the Gauss-Legendre method (figure 3b) employed by *thermofeel* to calculate MRT in the area surrounding North America (120W,20W,20S,60N) for the 42nd step after an initial date of 21 May 2021 around where the continent is experiencing it's maximum cossza value (figure 3c). Whilst there are up to -5K anomalies evident for North America (figure 3c). Notably the current operational calculation of MRT does not consider the continent of Antarctica (figure 3a) and as such this is cropped out in all output plots.

In addition, considering the medium range forecast for the initial date 21 May 2021 00UTC, the maximum positive anomaly is 19K. In comparison, the largest negative anomaly is -28K. However, the difference in the mean anomaly over all time steps is -1.5K. This demonstrates that the difference in the methods is more evident in the extremes of the distribution of MRT.

In comparison, the biggest difference for the UTCI mirrors the patterns seen for the MRT. There is around a +5K difference between the operational UTCI (figure 4a) and the *thermofeel* Gauss-Legendre UTCI (figure 4b) in areas around North America, where cossza is at its maximum (figure 4c). Whilst there is a -10K anomaly where cossza is at its maximum (figure 4c). When considering the medium range forecast for the initial date 21 May 2021 00UTC, the maximum positive anomaly is 6.6K, whereas the mean anomaly is -0.42K.

In addition, there is a noticeable difference between both MRT and UTCI values (figures 5 and 6) when dsrp is present in the calculation of MRT using *thermofeel* in comparison to when it is approximated using fdir and cossza (equation 7). The biggest difference is in Greenland at up to +17K for MRT (figure 5c) and +6K for the UTCI (figure 6c). For MRT at the 42nd time step after an initial date of 27 July 2021 the mean anomaly between the approaches is +2K, whilst the min is 0K and the max +17K. In comparison the mean anomaly at the same time step for UTCI is 0.62K, the min is also 0K and the max anomaly is 6.5K.

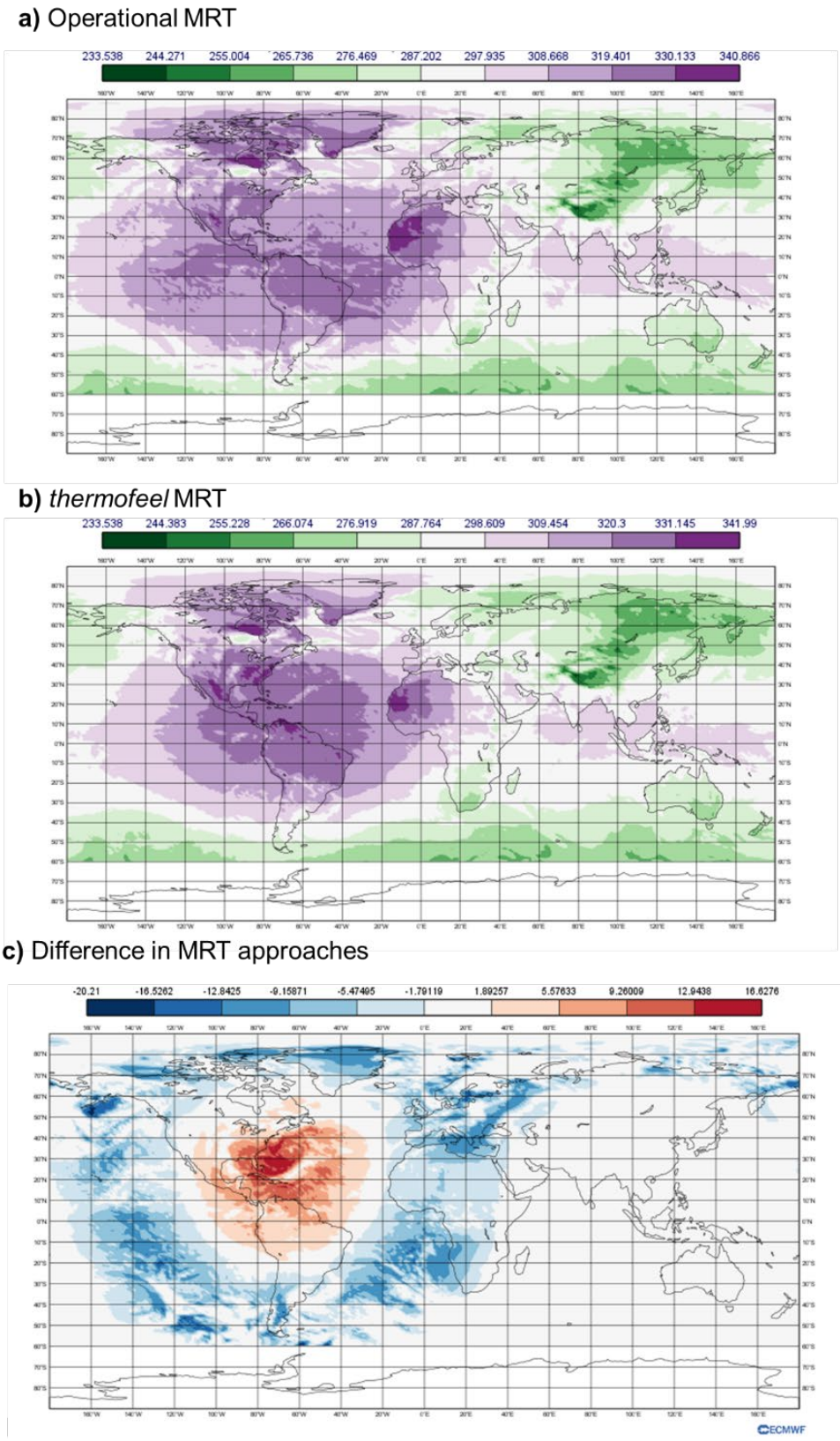

Figure 3: the operational c mean radiant temperature (top), the thermofeel mean radiant temperature (middle) and the anomaly plot of the approaches (bottom). For the 42nd step after the initial date 21 May 2021 at 00UTC.

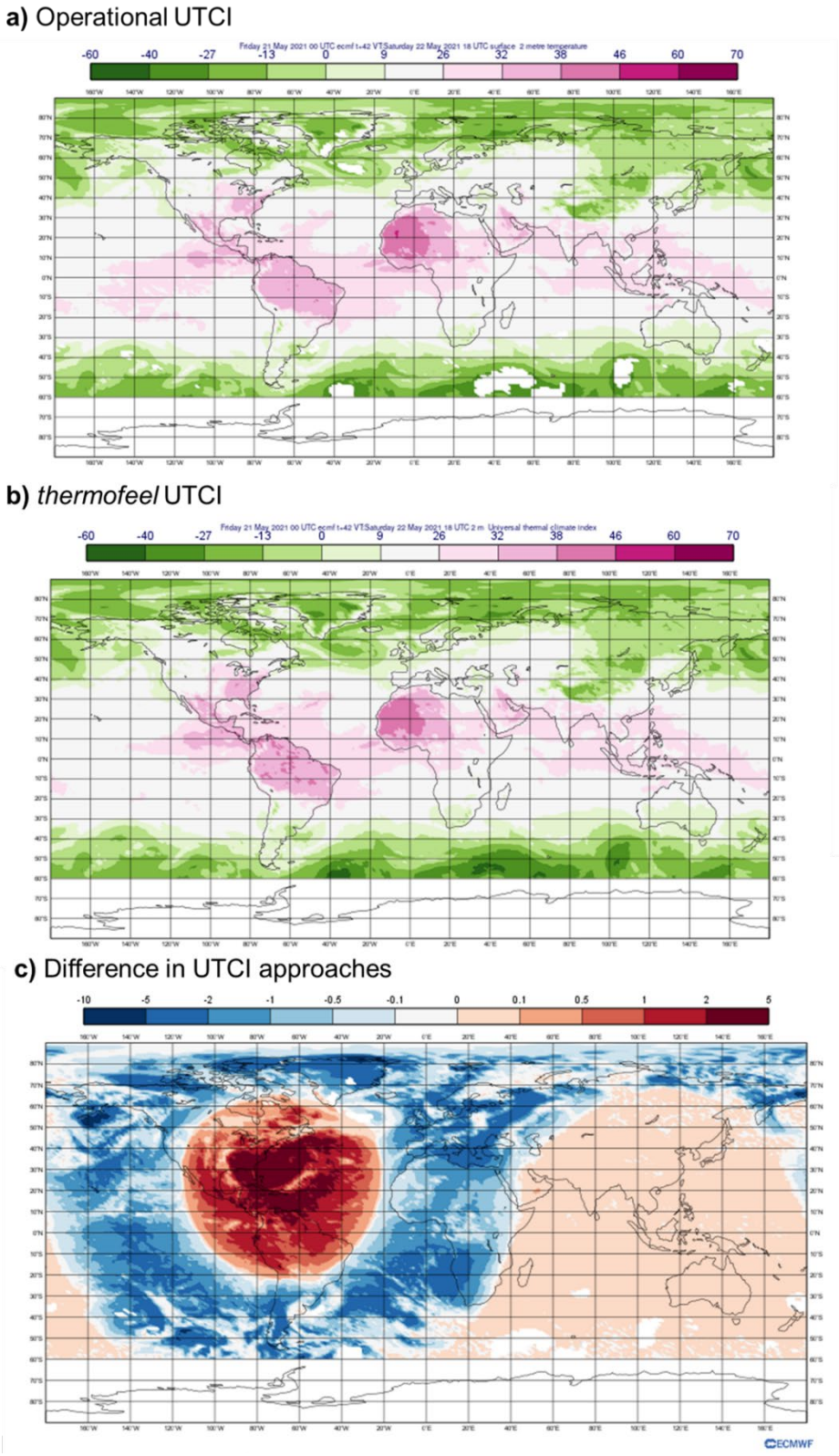

Figure 4: the operational c universal thermal climate index(top), the thermofeel universal thermal climate index (middle) and the anomaly plot of the approaches (bottom). For the 42nd step after the initial date 21 May 2021 at 00UTC.

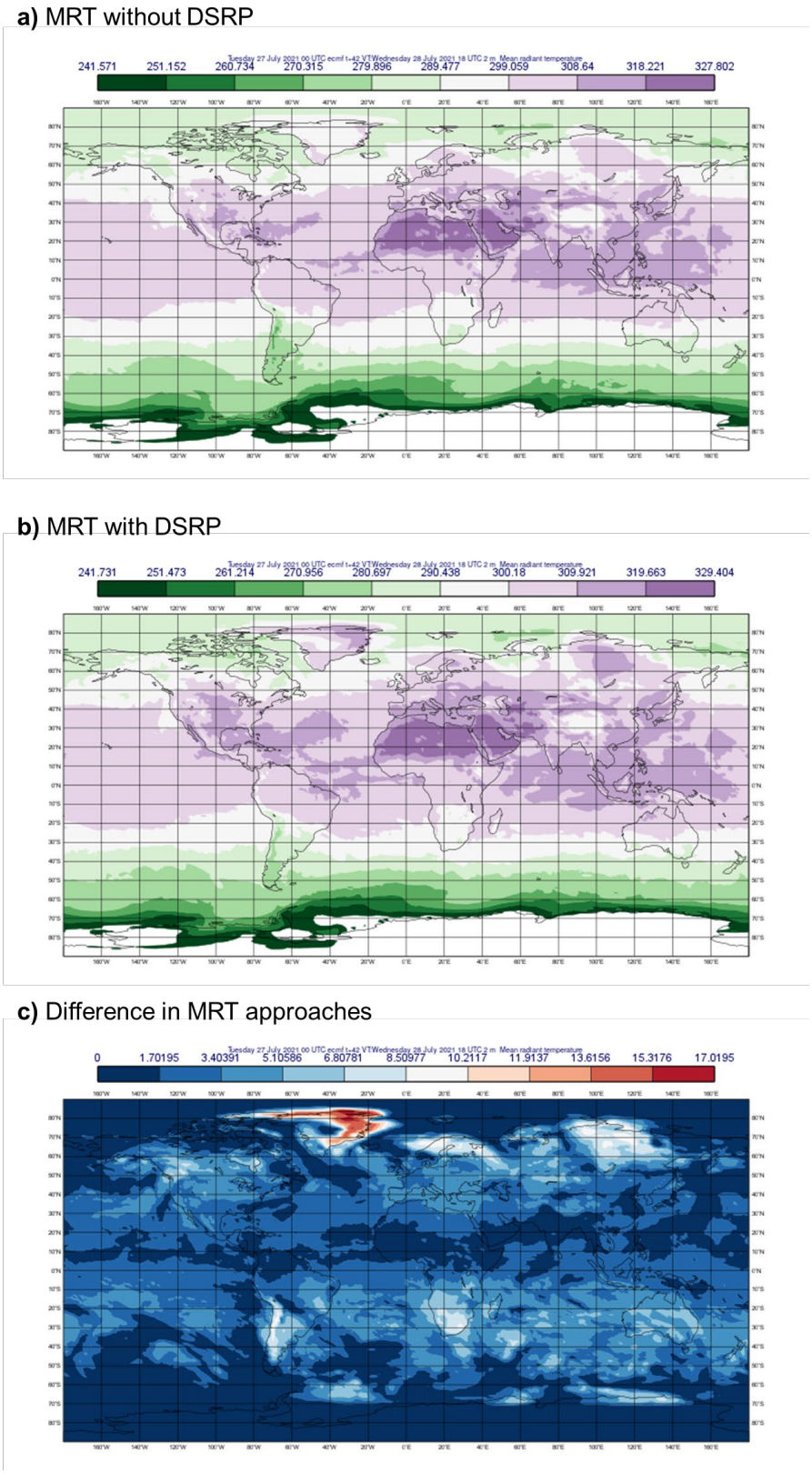

Figure 5: thermofeel MRT without dsrp(top), the thermofeel mean radiant temperature with dsrp (middle) and the anomaly plot of the approaches (bottom). For the 42nd step after the initial date 27 July 2021 at 00UTC.

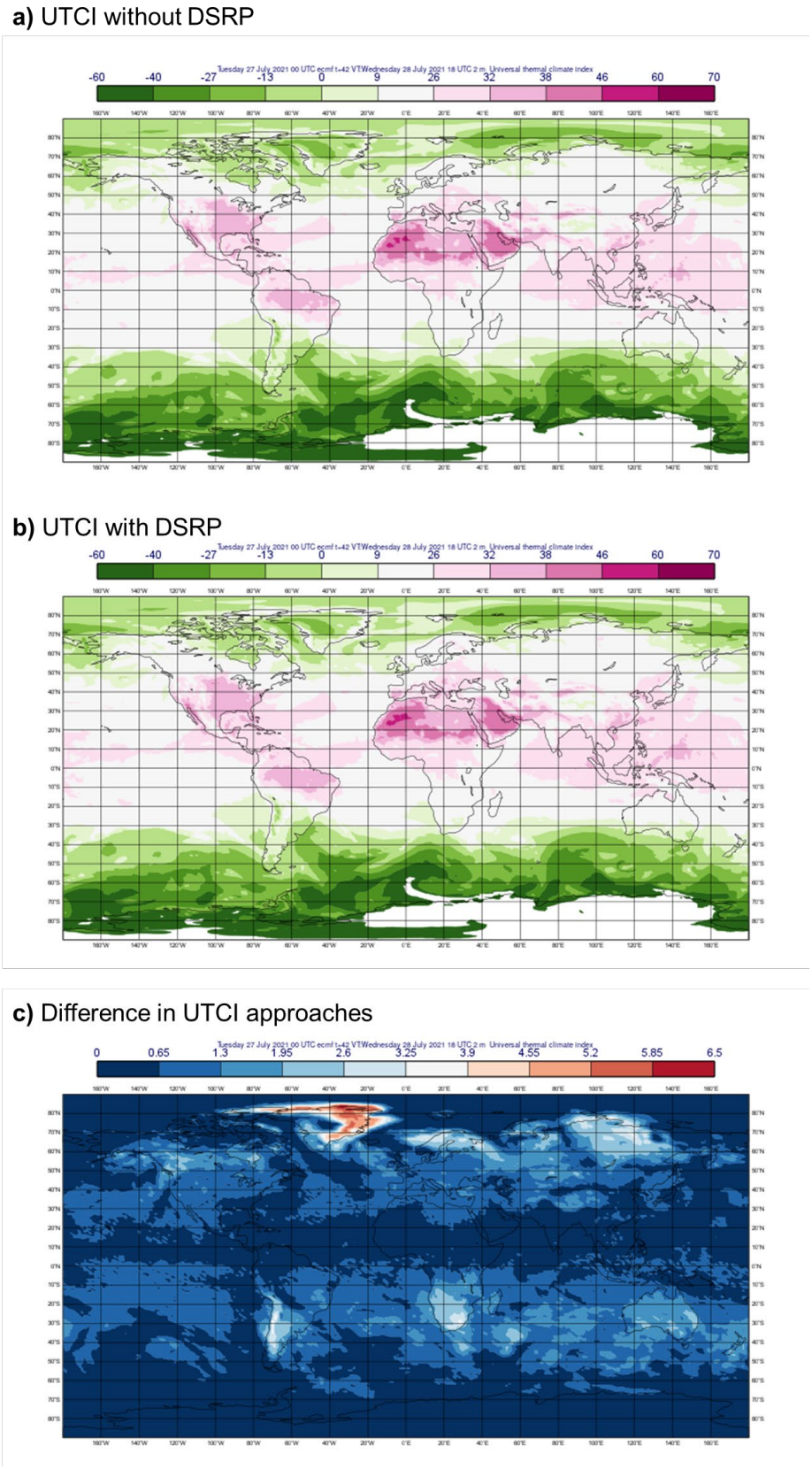

Figure 6: thermofeel UTCI from MRT without dsrp(top), the thermofeel UTCI from MRT with dsrp (middle) and the anomaly plot of the approaches (bottom). For the 42nd step after the initial date 27 July 2021 at 00UTC.

Discussion

We recommend that the Gauss-Legendre integrated cossza and the thermofeel methodology supersedes the operational c code used to calculate the ERA5-HEAT dataset. This is because the thermofeel method removes the clipping at the top of the parabola that is present in the c code (figure 2).

There is a substantial difference between the Gauss-Legendre integrated cossza employed in the thermofeel methodology to calculate MRT and UTCI in comparison to the operational c code currently creating the ERA5-HEAT dataset (Brimicombe et al., 2022; Di Napoli et al., 2021). This is more so evident in the extremes of the distribution of both UTCI and MRT. This suggests that the ERA5-HEAT dataset may be underestimating heat stress values while overestimating cold stress values, which could have implications for the health sector who can use heat stress forecasts to make lifesaving decisions (Blazejczyk et al., 2012; Jendritzky & Tinz, 2009; Di Napoli et al., 2019; Urban et al., 2021). The biggest difference is observed around where cossza is at its maximum (figure 3 and 4). However, the observed differences are larger when the step duration is bigger, and therefore the magnitude of error is less at 1 hour time step (i.e., ERA-5) in comparison to a 6 hourly forecast time step (i.e., after a 144-step). Further, there is a substantial difference between both MRT and UTCI values when dsrp is used in the place of fdir in the MRT calculation (equation 6 and 7).

We therefore recommend that if ERA5-HEAT is rereleased using the thermofeel methodology with fdir in the MRT calculation alongside the existing 'legacy' dataset available that the documentation indicates that differences are observed when dsrp is used in the place of fdir to be transparent with users. We recommend that the full forecast data is released as calculated using fdir for MRT using thermofeel to aid with decisions that are increasingly being made about thermal comfort conditions as a beta forecast and urge that dsrp be released in IFS (on all lead times) as a priority (Brimicombe et al., 2021, 2022).

In the ERA5-HEAT dataset Antarctica is currently cropped out and this is because of the many missing values that occur in this region (Di Napoli et al., 2021). We recommend that when the data is rereleased using the methodology introduced using the thermofeel library that Antarctica remains part of the dataset and that missing values and anomalous values are assigned as such, this is of benefit because it demonstrates to users that Antarctica does exist within the dataset but is often outside the range of the UTCI method (Bröde et al., 2012).

In addition, the UTCI and its components would benefit from a sensitivity analysis. We know that the windy and extreme cold conditions of Antarctica are outside the remit of the UTCI method, and previously it has been demonstrated that high MRT and low wind speeds lead to a higher UTCI values (Pappenberger et al., 2015), but, there is current understanding of which combination of the meteorological components of the UTCI (2m Air Temperature, MRT, Saturation Vapour Pressure and Wind Speed), lead to its hottest and coldest values. Such an analysis would allow us to better understand this thermal comfort index.

In addition, we suggest that the saturation vapour pressure method over ice is investigated in the calculation of saturation vapour pressure, a key component of the UTCI (Bröde et al., 2012; Hardy, 1998; Di Napoli et al., 2021). Currently the methodology for water saturation water vapour pressure is

used universally, whereas for colder regions where ice is present on the ground the optimum approach is slightly different (Hardy, 1998). This could be useful as it could make the values for Antarctica within the range of the UTCI method and allow cold stress to be considered, which is currently not always possible.

Conclusion

We have demonstrated that the *thermofeel* methodology for calculating the variables of cossza, mrt and utci should supersede the operational c code that creates the ERA5-HEAT dataset. We recommend that it is used to create an ERA5-HEAT version 2 beta and is published alongside the legacy dataset, allowing for users to make their own comparisons as well as, the full forecast dataset as beta. In addition, we urge that dsrp is made operational in IFS so that a more accurate MRT can be calculated for the forecasts from *thermofeel*. In addition, we recommend that Antarctica is no longer cropped from the dataset, allowing users to recognize where data is missing and where it is present. Further, we recommend a sensitivity analysis of the UTCI is carried out to improve understanding of what combinations of the meteorological components lead to the highest and lowest values. Finally, the saturation vapour pressure over ice should be explored for the continent of Antarctica. Overall, the method introduced in *thermofeel* will allow for ERA5-HEAT to be readily expanded to operational forecasts and other thermal comfort indices, benefitting many users of ECMWF data.

References

Aktaş, A., & Kirçiçek, Y. (2021). Examples of Solar Hybrid System Layouts, Design Guidelines, Energy Performance, Economic Concern, and Life Cycle Analyses. *Solar Hybrid Systems*, 331–349. https://doi.org/10.1016/B978-0-323-88499-0.00013-6

Babolian, E., Masjed-Jamei, M., & Eslahchi, M. R. (2005). On numerical improvement of Gauss-Legendre quadrature rules. *Applied Mathematics and Computation*, *160*(3), 779–789. https://doi.org/10.1016/j.amc.2003.11.031

Blazejczyk, K., Epstein, Y., Jendritzky, G., Staiger, H., & Tinz, B. (2012). Comparison of UTCI to selected thermal indices. *International Journal of Biometeorology*, *56*(3), 515–535. https://doi.org/10.1007/s00484-011-0453-2

Brimicombe, Chloe, Di Napoli, Claudia, Quintino, Tiago, Pappenberger, F., Cornforth, R., & Cloke, H. L. (2021). *thermofeel*. https://doi.org/https://doi.org/10.21957/mp6v-fd16

Brimicombe, Chloe, Di Napoli, Claudia, Quintino, Tiago, Pappenberger, Florian, Cornforth, Rosalind, & Cloke, H. L. (2022). thermofeel: a python thermal comfort indices library. *Software X*.

Bröde, P., Fiala, D., Błażejczyk, K., Holmér, I., Jendritzky, G., Kampmann, B., et al. (2012). Deriving the operational procedure for the Universal Thermal Climate Index (UTCI). *International Journal of Biometeorology*, *56*(3), 481–494. https://doi.org/10.1007/s00484-011-0454-1

De Dear, R. (1987). Ping-pong globe thermometers for mean radiant temperatures. *Heating and*

Ventilation Engineer and Journal of Air Conditioning, *60*, 10–11. Retrieved from https://ci.nii.ac.jp/naid/10030966825

Di Napoli, C., Pappenberger, F., & Cloke, H. L. (2019). Verification of Heat Stress Thresholds for a Health-Based Heat-Wave Definition. *Journal of Applied Meteorology and Climatology*, *58*(6), 1177–1194. https://doi.org/10.1175/jamc-d-18-0246.1

Di Napoli, C., Hogan, R. J., & Pappenberger, F. (2020). Mean radiant temperature from global-scale numerical weather prediction models. *International Journal of Biometeorology*, *64*(7), 1233–1245. https://doi.org/10.1007/s00484-020-01900-5

Di Napoli, C., Barnard, C., Prudhomme, C., Cloke, H. L., & Pappenberger, F. (2021). ERA5-HEAT: A global gridded historical dataset of human thermal comfort indices from climate reanalysis. *Geoscience Data Journal*

Fiala, D., Havenith, G., Bröde, P., Kampmann, B., & Jendritzky, G. (2012). UTCI-Fiala multi-node model of human heat transfer and temperature regulation. *International Journal of Biometeorology*, *56*(3), 429–441. https://doi.org/10.1007/s00484-011-0424-7

Goldstein, C. M. (1965). Numerical Integration by Gaussian Quadrature. *NASA Technical Memorandum*.

Guo, H., Teitelbaum, E., Houchois, N., Bozlar, M., & Meggers, F. (2018). Revisiting the use of globe thermometers to estimate radiant temperature in studies of heating and ventilation. *Energy and Buildings*, *180*, 83–94. https://doi.org/10.1016/j.enbuild.2018.08.029

Hardy, B. (1998). ITS-90 FORMULATIONS FOR VAPOR PRESSURE, FROSTPOINT TEMPERATURE, DEWPOINT TEMPERATURE, AND ENHANCEMENT FACTORS IN THE RANGE –100 TO +100 C Bob Hardy. *The Proceedings of the Third International Symposium on Humidity & Moisture*, (April), 1–8.

Hogan, R. J., & Hirahara, S. (2015). Effect of solar zenith angle specification on mean shortwave fluxes and stratospheric temperatures. *ECMWF Technical Memorandum*. Retrieved from http://www.ecmwf.int/en/research/publications

Hogan, R. J., & Hirahara, S. (2016). Effect of solar zenith angle specification in models on mean shortwave fluxes and stratospheric temperatures. *Geophysical Research Letters*, *43*(1), 482–488. https://doi.org/10.1002/2015GL066868

Jendritzky, G., & Tinz, B. (2009). The thermal environment of the human being on the global scale. *Global Health Action*. https://doi.org/10.3402/gha.v2i0.2005

Pappenberger, F., Jendritzky, G., Staiger, H., Dutra, E., Di Giuseppe, F., Richardson, D. S., & Cloke, H. L. (2015). Global forecasting of thermal health hazards: the skill of probabilistic predictions of the Universal Thermal Climate Index (UTCI). *International Journal of Biometeorology*, *59*(3), 311–323. https://doi.org/10.1007/s00484-014-0843-3

Thorsson, S., Rocklöv, J., Konarska, J., Lindberg, F., Holmer, B., Dousset, B. and Rayner, D., 2014. Mean radiant temperature–A predictor of heat related mortality. *Urban Climate*, *10*, pp.332-345.

Urban, A., Di Napoli, C., Cloke, H. L., Kyselý, J., Pappenberger, F., Sera, F., et al. (2021). Evaluation of the ERA5 reanalysis-based Universal Thermal Climate Index on mortality data in Europe.

Environmental Research, *198*, 111227. https://doi.org/10.1016/j.envres.2021.111227

Vanos, J. K., Rykaczewski, K., Middel, A., Vecellio, D. J., Brown, R. D., & Gillespie, T. J. (2021). Improved methods for estimating mean radiant temperature in hot and sunny outdoor settings. *International Journal of Biometeorology*, *65*(6), 967–983. https://doi.org/10.1007/S00484-021-02131-Y/FIGURES/6

Zienkiewicz, O.C., Taylor, R.L. and Zhu, J.Z., 2005. *The finite element method: its basis and fundamentals*. (pg. 160) Elsevier.